Ionization-Induced Self-Compression of Tightly Focused Femtosecond Laser Pulses

Z.-H. He, J. A. Nees, B. Hou, K. Krushelnick, and A. G. R. Thomas
Center for Ultrafast Optical Science, University of Michigan, Ann Arbor, Michigan 48109, USA
(Received 17 July 2014; published 30 December 2014)

As lasers become progressively higher in power, optical damage thresholds will become a limiting factor. Using the nonlinear optics of plasma may be a way to circumvent these limits. Here, we present a new self-compression mechanism for high-power, femtosecond laser pulses based on geometrical focusing and three dimensional spatiotemporal reshaping in an ionizing plasma. By propagating tightly focused, 10-mJ femtosecond laser pulses through a 100-μm gas jet, the interplay between ionization gradients, focusing, and diffraction of the light pulse leads to stable and uniform self-compression of the pulse, while maintaining a high-energy throughput and excellent refocusability. Self-compression down to 16 fs from an original 36-fs pulse is measured using second-harmonic-generation frequency-resolved optical gating. Using this mechanism, we are able to maintain a high transmission ($> 88\%$) such that the pulse peak power is doubled. Three-dimensional numerical simulations are performed to support our interpretation of the experimental observations.

DOI: 10.1103/PhysRevLett.113.263904 PACS numbers: 42.65.Re, 52.25.Jm, 52.38.-r

Understanding the propagation of intense femtosecond laser pulses in gases and/or underdense plasmas is of crucial interest in areas such as laser driven particle acceleration [1] and attosecond pulses from high harmonic generation [2]. The nonlinear interaction of laser pulses in a transparent medium is also useful for applications in generating ultrashort pulses at high energy levels via temporal compression. Although conventional Ti:sapphire based amplifier systems are currently able to generate laser pulses at joule level energies, the pulse duration is typically limited to 25 fs or greater by the gain-narrowing effect in the amplifier medium and imperfect dispersion compensation. Kerr induced self-phase-modulation and/or ionization-induced nonlinearity have previously been used as sources of spectral broadening for postcompression in plasma filaments [3,4], gas-filled waveguides [5], or bulk media [6].

A relativistically intense pulse driving a plasma wave can also lead to self-compression [7–14]. However, it is a challenging problem to achieve homogenous temporal pulse compression with a focusable spatial profile and high-energy throughput efficiency. In addition, demonstration of a high degree of stability is of great importance.

Ionization induced spectral broadening [15] for postcompression has become an attractive idea in several recent studies [16–20] because of its potential to scale to high-energy pulses and overcome the energy limit typically found in self-phase-modulation and filamentation methods. However, since ionization also results in a transverse refractive index variation, an external guiding structure, such as a large diameter capillary waveguide, is required for moderate interaction lengths (typically on the order of 10 cm). Additional dispersion compensation using dispersive optical elements such as chirped mirrors [21] may still be necessary at the output of the waveguides [16,17]. Alternatively, the dispersion can be self-compensated via spatiotemporal reshaping inside capillaries [18,19], which results in self-compression of the laser pulse.

In this Letter, we present experimental results and three-dimensional (3D) particle-in-cell (PIC) simulations demonstrating self-compression of a 10-mJ laser pulse in plasma using a relatively tight focusing scheme without any external guiding structures, operating at high intensities in the weakly relativistic plasma regime with $a_0 \sim 1$, where $a_0 = eA/m_e c$ is the normalized vector potential (approximately 2×10^{18} W/cm^{-2} for 790 nm light). The combination of ionization induced refraction, focusing, and diffraction in 3D space lead to stable and reproducible compression from 36 to 16 fs with good spatial mode quality. Our simulations indicate that spectral broadening can be mainly attributed to optical-field-ionization. The complicated dispersion of the higher-order modes generated by the ionization gradients results in compression, similar to the results in Ref. [18] but without a waveguide. The high transmission means that the pulse peak power is nearly doubled. Two of the key requirements to achieve this are the use of a very short ($\sim$100 μm) moderate density ($n_e \sim 10^{19}$ cm^{-3}) free-flowing gas jet and relatively large numerical aperture focusing ($f/2$), which enable significant compression to occur without a guiding structure. This method does not suffer from limitations due to coupling efficiency or material damage present in guided geometries, thus, it can be easily implemented at high-repetition rates and should be scalable to much higher powers.

The experiments were carried out using the high-repetition-rate λ^3 laser system at the University of Michigan—a table-top subterawatt Ti:sapphire laser system that delivers up to 10-mJ, 35-fs pulses at a central wavelength of 790 nm at 0.5-kHz repetition rate. The linearly

polarized laser beam was focused by an $f/2$ off-axis parabolic mirror onto an expanding gas flow produced from a 100-μm diameter nozzle. A deformable mirror was used to correct the wavefront and obtain the highest intensity laser spot. The gas density was varied by setting the backing pressure. A turbomolecular vacuum pump was placed above the continuously flowing gas nozzle to maintain an equilibrium state during the experiments. Plasma electron density was determined by interferometry using a transverse probe beam. The on-axis density profile exhibited a Gaussian distribution with full width at half maximum (FWHM) in the range 150–300 μm, depending on the distance from the focus to the nozzle orifice.

Light transmitted through the focus was collimated by a second parabolic mirror and transported out of the vacuum chamber through a 500-μm-thick fused silica Brewster window. The energy of the output pulse was measured by an optical power meter (Coherent PM30). Alternately, the collimated light was reflected by a wedged plate onto a diffuser screen for near-field mode imaging or an $f/1$ parabolic mirror to characterize its focusability. An iris diaphragm was inserted to limit the beam profile for alignment of temporal characterization in a commercial single-shot second-harmonic-generation (SHG) frequency-resolved optical gating (FROG) device [22]. Optical spectra were independently recorded using a miniature spectrometer (Ocean Optics USB4000), with the absolute spectral response across all wavelengths being calibrated *in situ* for our imaging setup using a white light source.

The laser intensity along the propagation axis was calculated based on the f number of the focusing optics used in the experiments for vacuum propagation. Ideal diffraction-limited focusing was assumed and was used only to provide a reasonable estimate for the laser intensities in the intermediate region near the focus but not the peak intensity at focus because of imperfections and aberrations of the optical systems. A deformable mirror can be used to correct wavefront distortion to produce a close-to-diffraction-limited focal spot [23]. It is, however, found that the pulse compression was not sensitive to having an optimized spot at the far-field plane since we employed the ionization nonlinearity in the midfield region.

Figure 1 shows the measured FWHM pulse durations as a function of the focal position. The minimum output pulse duration was found with the gas jet placed at 0.2 mm (0.3 mm) and 0.4 mm (0.6 mm) after (before) the geometrical focus for He and H_2 gas, respectively. The pulse compression was associated with spectral broadening, clearly depicted in Figs. 1(a) and 1(b), where a large blueshift of the central wavelength occurs at the optimal compression points. The broadening is a consequence of new frequency components generated in the blue-shifted spectrum during optical field ionization. The influence of the gas species can be explained by the different ionization potentials for helium and hydrogen atoms.

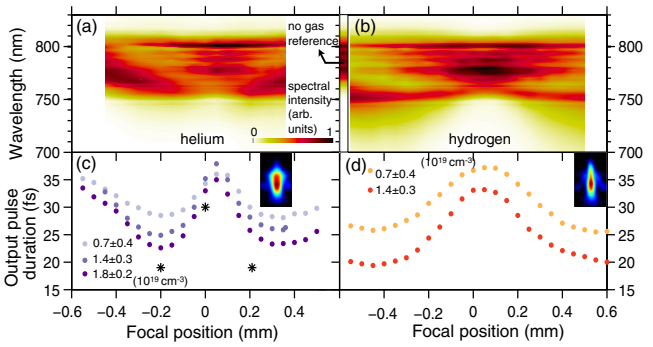

FIG. 1 (color online). Composite images showing the measured optical spectra as a function of the focus position for helium (a) and hydrogen (b) at the same peak plasma density of $(1.4 \pm 0.3) \times 10^{19}$ cm^{-3}. A reference spectrum obtained without gas is also shown. Output pulse duration (FWHM) as a function of the focal position for (c) helium and (d) hydrogen at various plasma densities, obtained using different backing pressures (4.5, 6.6, and 9.0 bar for helium; 4.5 and 6.7 bar for hydrogen). The measured FROG traces are shown in the corresponding insets for helium at 22 fs and hydrogen at 20 fs. The initial pulse duration was 38 fs for this data set. The three data points (black asterisk) plotted in (c) are taken from results of 3D PIC simulations.

The laser intensities corresponding to the barrier suppression ionization [24] threshold for hydrogen and helium (the first ionization charge state) are 1.4×10^{14} W/cm^{-2} and 1.5×10^{15} W/cm^{-2}, respectively. Given one focusing position and gas type, the spectral bandwidth increases with the backing pressure (gas density), which gives more temporal compression. A similar trend was also observed using argon gas, with a distance of approximately 0.15 mm (0.2 mm) after (before) the focus for optimal compression.

Although more complex dynamics can be expected due to multi-ionization (successive ionization charge states up to 8 are achievable under our experiment conditions), we found that the compression was relatively insensitive to the gas species over a range of similar plasma densities. Here, the focus position was fixed where the compression point was optimized using argon gas at the greatest plasma densities. No measurement was made with helium gas above a plasma density of 7×10^{19} cm^{-3}; a fourfold increase in backing pressure was required for helium to provide the same plasma electron density compared to argon, thus, the gas flow may give a larger interaction volume. Further increase of the gas backing pressure was observed to cause pulse-to-pulse instability and strong modulation in the transmitted beam profile. Moreover, FROG measurement became unreliable as the measured spectrum continued to become blueshifted and reached the bandwidth limit of the nonlinear crystal in the FROG device (a 30 μm thick β-barium borate crystal), because the SHG efficiency becomes lower at shorter wavelengths. FROG retrieval errors [root-mean-square (RMS) difference

between the experimental and retrieved traces] were below 2% on a 128×128 grid for all measurements reported in this Letter.

The shortest stable pulse we measured was of 16-fs duration with argon gas. Figure 2 shows the FROG data with and without gas. The initial pulse [Fig. 2(a)] with a duration of 36 fs FWHM was self-compressed to a near-transform-limited pulse of 16 fs [Fig. 2(b)] under optimal conditions. Some slight variation of the original pulse duration reported in this Letter was due to day-to-day alignment of amplifiers of the laser system and the configuration of a front-end spectral amplitude and phase filter (Dazzler, Fastlite).

In Fig. 2(d) we show that our measurements are consistent, by comparing the measured and retrieved spectra from the FROG. Fluctuations smaller than 0.4 fs RMS were observed for the FWHM pulse duration at 16 fs. Asymmetric spectral broadening with a large blue shifted component was measured for the compressed pulse. The absence of significant frequency downshifting (indicative of large amplitude plasma wave excitation) suggests that even higher energy efficiency might be achieved because the laser pulse is not losing energy in generating a large amplitude plasma wakefield and the subsequent trapping of energetic electrons as in the strong nonlinear relativistic regime [11,12].

On the other hand, previous compression work employing a much lower laser intensity using the filamentation processes suffered losses due to multiphoton ionization over long propagation, thus, limiting the energy efficiency. By contrast, in the operating regime of our experiments, the peak laser intensity increased or decreased rapidly with propagation distance, and optical-field-ionization occurs in the leading fraction of the pulse over a very short distance ($\sim$100 μm). Indeed, we find a high total energy transmission (88% for the measurement in Fig. 2) by measuring the pulse energy using a power meter. The transmission was increased to 95% at half the backing pressure, but with a lower level of compression. Moreover, our scheme is free of an external guiding structure, which eliminates any loss in compression efficiency due to imperfect coupling seen in previous studies.

The maximum peak plasma density used was a few 10^{19} cm^{-3} such that the near field mode of the transmitted light remained stable from shot to shot with good spatial quality. Ionization instability [25] may become important at much higher densities, where we observed strong modulation on the beam profile. However, we also confirmed that the temporal compression may be considered homogenous by measuring various locations across the beam. The resulting FROG traces are almost identical, with less than 2 fs difference in the retrieved FWHM pulse durations at all transverse locations. The transmission spectra obtained using the different parts exhibit essentially identical blue-shifting and modulation after normalization, indicating the nonlinear processes are uniform across the transverse beam.

The beam profiles of a stable compressed pulse are shown in Fig. 3(b) to have a relatively smooth spatial mode. There is some modulation to the spatial profile introduced by the plasma; in the insets of Fig. 3, we show that the refocused spot shape does not change significantly from the vacuum case to that with flowing argon gas, demonstrating excellent focusability of the transmitted beam. In both "no gas" and "with gas" cases, the optical imaging system was identical. This implies that the peak intensity can effectively be doubled after the compression. Since the process is stable, the use of adaptive optics after the pulse compression can effectively correct any additional wavefront distortions [23]. This demonstration of the stability

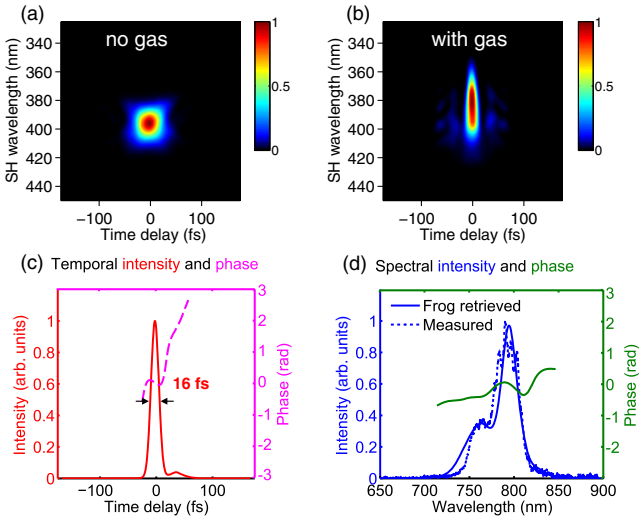

FIG. 2 (color online). The FROG traces measured at the output (a) with no gas and (b) with gas (argon) after self-compression. (c)–(d) The retrieved temporal and spectral intensity and phase for the self-compressed pulse. The retrieval error is 0.016 on a 128×128 grid. The measured spectrum (dotted curve) is plotted in (d) for comparison with the FROG retrieved spectrum.

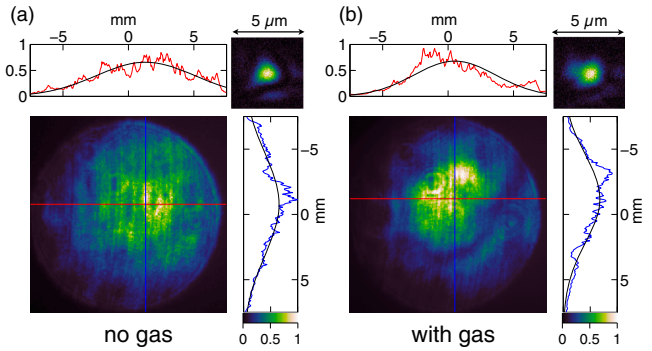

FIG. 3 (color online). The measured near-field profiles of the transmitted beam (a) with no gas and (b) with argon at a backing pressure of 12 bar. The refocused beam profiles are shown in the top right insets. Lineouts represent the least squares fitting results of the measured profile using a 2D Gaussian function.

and focusability is clearly important for the plasma based compression to be a practical technique.

To interpret our experiment results, we have performed a series of 3D PIC simulations using the OSIRIS 2.0 framework [26]—a fully explicit relativistic electromagnetic particle-in-cell code that includes a suite of ionization physics models. The PIC approach contains the full range of electromagnetic and collisionless plasma physics, yet the nonlinear response of bound electrons in atoms and molecules such as the Kerr effect is not included in the codes. The ionization rate typically increases very rapidly with laser intensity. It should be pointed out that for the given scale length of the gas profile in our experiments, the self-phase-modulation contributed by Kerr nonlinearity can be considered negligible when compared to the change of refractive index induced by ionization [27]. This validates the use of PIC codes to model our experiments.

Simulations were carried out in a moving window of the dimensions $64 \times 230 \times 230\ \mu\text{m}^3$ on a Cartesian grid with step sizes $\Delta x_1 = \lambda/10$ (the propagation direction) and $\Delta x_2 = \Delta x_3 = \lambda/3$ (the transverse direction). The transverse extent was chosen to be sufficient to contain the large diffraction angle of a tightly focused laser beam. Ionization physics was implemented using an Ammosov-Delone-Krainov tunnel ionization model [28]. For each ionization level, particles with a charge-to-mass ratio equivalent to that of an electron were used, with $2 \times 2 \times 2$ particles per cell. The neutral density profile has a truncated Gaussian profile with a FWHM width of 150 μm.

The reshaping dynamics of an ionizing laser pulse was first studied using numerical models based on nonlinear envelope propagation for a two-dimensional pulse [29], where it was shown that the light pulse can transform into a horseshoe or horn-type structure during its ionization process. Similar ionization induced refraction was also measured experimentally by Chessa *et al.* in [30].

Figure 4 illustrates the evolution of the laser pulse structure at different propagating distances taken from a 3D simulation for the scenario when a neutral helium gas density profile is peaked 200 μm before the geometric focus (at 500 μm). The maximum neutral gas density is $0.02n_c$, corresponding to an electron density of $0.04n_c$ when fully ionized. To visualize the local change of the laser spectrum, the frequency shift distribution at the center slice for the laser polarization plane is plotted, with a cutoff threshold at 10% of the maximum intensity, below which the frequency shift is not shown.

As can be seen from the local frequency shift, a large leading part of the pulse gradually becomes blueshifted as a result of optical field ionization during propagation through the helium gas around 300 μm. The laser pulse experiences a dramatic nonlinear refraction due to the rapidly changing refractive index induced by the increasing electron density. In the meantime, as the pulse converges towards focus, a dynamic redistribution of the pulse energy takes place,

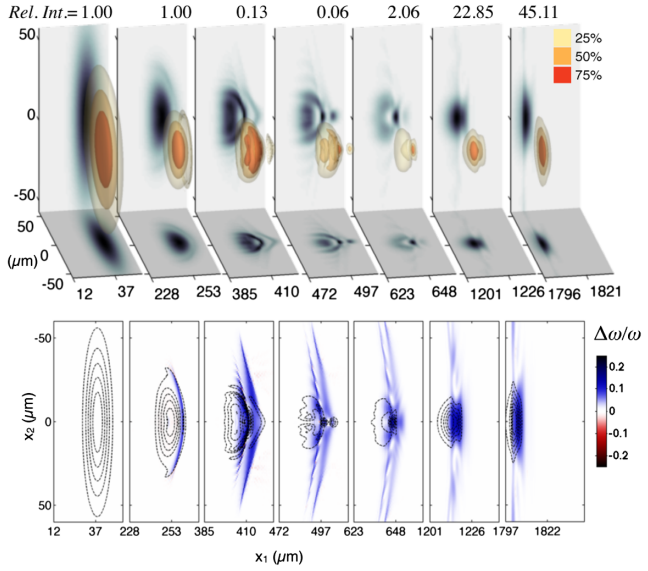

FIG. 4 (color online). The gas peak density is before the laser focus ($Z = 0.2$ mm). Top panel: isosurface plots (25%, 50%, and 75% of the maximum intensity) showing the pulse dynamics at different propagating distances. The relative intensity (Rel. Int.) is defined as the ratio of the peak intensity to that of a pulse propagating in vacuum. Side panels display intensity profiles at cross-sectional planes through the center of the box. Bottom panel: spatial distribution of the local frequency shift $\Delta\omega/\omega_0$ of the laser pulse for the center slice. The blue color represents frequency upshift (blueshift) and red for frequency downshift (redshift). The dashed lines are the 2D contour plots for the intensity profiles.

which leads to not only an enhanced peak intensity, but also a shorter temporal duration. Although multiple structures are observed during this complex interaction, diffraction into vacuum results in a single mode containing most of the pulse energy. Experimentally, the pulse splitting is often associated with an increased backing pressure and/or use of a gas species with multiple ionization levels. Sequential ionization is also known to cause self-phase-modulation of the laser pulse.

In simulations with the laser focused at the center of the density profile, only a small part at the leading edge of the pulse is involved with ionization. As a result, no significant blueshifting takes place within the body of the pulse, which corroborates our experimental observation in Fig. 1 that less spectral broadening is found when the gas jet is centered near the geometrical focus. However, it should be noted that, as the peak laser intensity approaches and exceeds the relativistic intensities ($a_0 \gtrsim 1$), excitation of plasma waves is possible, which can also give rise to pulse compression [31]. In this case, nonlinear shaping from ionization is much weaker compared to Fig. 4. Although the laser has a larger peak intensity near the focal region because of the absence of pulse splitting and strong nonlinear shaping, it experiences less longitudinal compression at the end of the simulation with a smaller peak

intensity at equivalent propagation distances. The pulse durations from these simulations for three different focal positions are plotted in Fig. 1(c), showing qualitative agreement with the experimental trend. They are taken at an identical propagation distance of 1.6 mm, before the pulse in one of the three cases reaches the boundary of the simulation box. The pulse in Fig. 4 finally transforms into one having a FWHM duration of 10 fs.

In conclusion, we have demonstrated efficient self-compression of a multi-mJ laser pulse by ionization induced reshaping of laser pulses in a 100-μm scale length continuously flowing gas target. This leads to very stable and reproducible compression down to 16 fs at a 0.5-kHz repetition rate without a guiding structure. The high transmission means that the pulse peak power is doubled. The consequences are twofold. First, we have demonstrated a practical way to achieve significant pulse shortening for high-field experiments. Second, the stability and scalability of the process indicates that plasma may be viable as a nonlinear optical medium to replace conventional optics in future high-power laser systems.

This work was funded by the NSF under Grants No. 0903557 and No. 1054164, the AFOSR Young Investigator Program under Grant No. FA9550-12-1-0310 and DARPA under Contract No. N66001-11-1-4208. The authors acknowledge the OSIRIS Consortium, consisting of University of California, Los Angeles (UCLA) and Instituto Superior Técnico (IST) (Lisbon, Portugal), for the use of the OSIRIS 2.0 framework. This research was supported in part through computational resources and services provided by Advanced Research Computing at the University of Michigan, Ann Arbor.

[1] E. Esarey, C. B. Schroeder, and W. P. Leemans, Rev. Mod. Phys. **81**, 1229 (2009).
[2] F. Krausz and M. Ivanov, Rev. Mod. Phys. **81**, 163 (2009).
[3] A. Couairon and A. Mysyrowicz, Phys. Rep. **441**, 47 (2007).
[4] A. Mysyrowicz, A. Couairon, and U. Keller, New J. Phys. **10**, 025023 (2008).
[5] M. Nisoli, S. D. Silvestri, O. Svelto, R. Szipöcs, K. Ferencz, C. Spielmann, S. Sartania, and F. Krausz, Opt. Lett. **22**, 522 (1997).
[6] V. Chvykov, C. Radier, G. Cheriaux, G. Kalinchenko, V. Yanovsky, and G. Mourou, in *2010 Conference on Lasers and Electro-Optics (CLEO) and Quantum Electronics and Laser Science Conference (QELS), 16–21 May 2010* (IEEE, Piscataway, NJ, 2010), pp. 1–2.
[7] F. S. Tsung, C. Ren, L. O. Silva, W. B. Mori, and T. Katsouleas, Proc. Natl. Acad. Sci. U.S.A. **99**, 29 (2002).
[8] C. Ren, B. J. Duda, R. G. Hemker, W. B. Mori, T. Katsouleas, T. M. Antonsen, and P. Mora, Phys. Rev. E **63**, 026411 (2001).
[9] O. Shorokhov, A. Pukhov, and I. Kostyukov, Phys. Rev. Lett. **91**, 265002 (2003).
[10] D. F. Gordon, B. Hafizi, R. F. Hubbard, J. R. Peñano, P. Sprangle, and A. Ting, Phys. Rev. Lett. **90**, 215001 (2003).
[11] J. Faure, Y. Glinec, J. J. Santos, F. Ewald, J.-P. Rousseau, S. Kiselev, A. Pukhov, T. Hosokai, and V. Malka, Phys. Rev. Lett. **95**, 205003 (2005).
[12] J. Schreiber, C. Bellei, S. P. D. Mangles, C. Kamperidis, S. Kneip, S. R. Nagel, C. A. J. Palmer, P. P. Rajeev, M. J. V. Streeter, and Z. Najmudin, Phys. Rev. Lett. **105**, 235003 (2010).
[13] A. A. Balakin, A. G. Litvak, V. A. Mironov, and S. A. Skobelev, Europhys. Lett. **100**, 34002 (2012).
[14] A. Pipahl, E. A. Anashkina, M. Toncian, T. Toncian, S. A. Skobelev, A. V. Bashinov, A. A. Gonoskov, O. Willi, and A. V. Kim, Phys. Rev. E **87**, 033104 (2013).
[15] W. M. Wood, C. W. Siders, and M. C. Downer, Phys. Rev. Lett. **67**, 3523 (1991).
[16] C. F. Dutin, A. Dubrouil, S. Petit, E. Mével, E. Constant, and D. Descamps, Opt. Lett. **35**, 253 (2010).
[17] T. Auguste, O. Gobert, C. F. Dutin, A. Dubrouil, E. Mével, S. Petit, E. Constant, and D. Descamps, J. Opt. Soc. Am. B **29**, 1277 (2012).
[18] N. L. Wagner, E. A. Gibson, T. Popmintchev, I. P. Christov, M. M. Murnane, and H. C. Kapteyn, Phys. Rev. Lett. **93**, 173902 (2004).
[19] S. A. Skobelev, A. V. Kim, and O. Willi, Phys. Rev. Lett. **108**, 123904 (2012).
[20] O. Hort, A. Dubrouil, C. Fourcade-Dutin, S. Petit, E. Mével, D. Descamps, and E. Constant, EPJ Web Conf. **41**, 10021 (2013).
[21] R. Szipöcs, C. Spielmann, F. Krausz, and K. Ferencz, Opt. Lett. **19**, 201 (1994).
[22] R. Trebino, K. W. DeLong, D. N. Fittinghoff, J. N. Sweetser, M. A. Krumbugel, B. A. Richman, and D. J. Kane, Rev. Sci. Instrum. **68**, 3277 (1997).
[23] O. Albert, H. Wang, D. Liu, Z. Chang, and G. Mourou, Opt. Lett. **25**, 1125 (2000).
[24] S. Augst, D. D. Meyerhofer, D. Strickland, and S. L. Chint, J. Opt. Soc. Am. B **8**, 858 (1991).
[25] T. M. Antonsen and Z. Bian, Phys. Rev. Lett. **82**, 3617 (1999).
[26] R. Fonseca, L. Silva, F. Tsung, V. Decyk, W. Lu, C. Ren, W. Mori, S. Deng, S. Lee, T. Katsouleas, and J. Adam, in *Computational Science—ICCS 2002*, edited by P. Sloot, A. Hoekstra, C. Tan, and J. Dongarra, Lecture Notes in Computer Science Vol. 2331 (Springer, Berlin, 2002), pp. 342–351.
[27] J. K. Wahlstrand, Y.-H. Cheng, and H. M. Milchberg, Phys. Rev. Lett. **109**, 113904 (2012).
[28] M. V. Ammosov, N. B. Delone, and V. P. Krainov, Sov. Phys. JETP **64**, 1191 (1986).
[29] A. Sergeev, E. Vanin, L. Stenflo, D. Anderson, M. Lisak, and M. L. Quiroga-Teixeiro, Phys. Rev. A **46**, 7830 (1992).
[30] P. Chessa, E. De Wispelaere, F. Dorchies, V. Malka, J. R. Marquès, G. Hamoniaux, P. Mora, and F. Amiranoff, Phys. Rev. Lett. **82**, 552 (1999).
[31] Z.-H. He, J. A. Nees, B. Hou, K. Krushelnick, and A. G. R. Thomas, Plasma Phys. Controlled Fusion **56**, 084010 (2014).